Acta Cryst. (1967). **23**, 1

The 'Memory Effect' in Silver Iodide*

BY G. BURLEY†

Institute for Materials Research, National Bureau of Standards, Washington, D.C., U.S.A.

(*Received* 11 *October* 1965 *and in revised form* 4 *November* 1966)

Radial distribution and least-squares site occupation analyses were performed on powder diffraction patterns of the high temperature phase of silver iodide taken at 155 and 250°C. A preferential occupation of certain sites by the silver atoms occurs near the transition temperature at 147°C, involving the silver atom positions nearest to those in the low-temperature wurtzite- and sphalerite-type structures respectively. The regeneration of a particular derivative low-temperature structure is thus facilitated, and a crystallographic explanation can be given for the observed 'memory effect'.

Introduction

Silver iodide is trimorphic at atmospheric pressure. Both a hexagonal (wurtzite type) structure and a metastable face-centered cubic (sphalerite type) structure can coexist to 147°C. At this temperature both convert to a high temperature body-centered cubic structure, which persists to the melting point of 555°C (Burley, 1963). The structure of this phase has been described by Strock (1934, 1936) in terms of a regular iodine framework and a statistically disordered arrangement of silver atoms.

Heating of either of the two low-temperature phases of silver iodide, or of mixtures, through the phase boundary into the stability region of the high-temperature phase, followed by cooling, results in regeneration of the original phase composition. This has been referred to as a 'memory effect' in the literature (Bloch & Moeller, 1931). No satisfactory explanation for this phenomenon has previously been advanced. Nucleation and recrystallization are unlikely for the following reasons: (1) No trace of either of the low-temperature phases can be seen above 147°C on the heating stage of an optical microscope. (2) The transition occurs extremely rapidly and reversibly, regardless of the rate of heating or cooling. (3) The integrated intensities for certain diffraction lines in the pattern for the high-temperature phase differ considerably near the transition temperature, depending only on the original phase composition. (4) The 'memory effect' persists even when the sample has been kept at temperatures between 150 and 155°C for several days. A slow shift toward the stable hexagonal phase does, however, occur during cooling.

Experimental

All experimental work was carried out with polycrystalline samples because (1) it has not been possible to grow single crystals of the low-temperature sphalerite-type phase and (2) a 6% volume decrease occurs at the transition to the high-temperature phase, which shatters a single crystal into fragments.

Nearly pure samples of the hexagonal phase of silver iodide were prepared by precipitation from solutions containing an excess of iodide ions. The face-centered cubic phase was prepared from this by application of hydrostatic pressure of 10–20 bars at room temperature. Experimental work was carried out on a high-temperature powder diffraction furnace, mounted on a high-angle diffractometer. Samples were heated to 155 ± 3°C and kept at that temperature for the entire duration of a run. The angular range from 0° to 80° in 2θ was scanned with both Cu $K\alpha$ and Mo $K\alpha$ radiations and the balanced filter technique. Further runs were made on the same sample on successive days. Starting materials were the pure hexagonal and face-centered cubic phases, as well as mixtures of the two. Additional runs were made on all samples at 250 ± 5°C, either initially or at the conclusion of the above-described work.

Preferred orientation effects, although ordinarily not very pronounced for silver iodide, were minimized by using very small crystallites and special sample preparation techniques. The low-temperature diffraction patterns were also compared against the calculated intensities. All of the included data showed deviations smaller than the limits of error for the low order reflections. Similar criteria were used at the conclusion of each run to insure that no orientation effects were introduced by the heating cycles.

The results can be summarized as follows: (1) Above 147°C, the diffraction patterns from all samples, regardless of temperature or initial phase composition, showed Bragg maxima at the same positions and could be indexed on the basis of a body-centered cubic unit cell, $a = 5{\cdot}02$ at 155°C. (2) No trace of the diffraction patterns of the low-temperature phases was discernible. (3) Pronounced differences existed between integrated intensities for the same reflection obtained from different starting materials (Table 1) at temperatures from 147 to about 165°C. (4) Integrated intensities for the

---

* Research supported by the Atmospheric Sciences Program, National Science Foundation, NSF Grant G19648.

† Present address: U.S. Atomic Energy Commission, Division of Reactor Licensing, Bethesda, Md., U.S.A.

same reflection, regardless of previous history, were identical in the patterns taken at 250°C and in agreement with the results of Strock (1936) and Hoshino (1957). (5) Considerable temperature diffuse scattering was evident in all patterns, but more pronounced in those taken at 250°C. (6) The 'memory effect' becomes irreversibly erased at temperatures above 170–175°C. Heating above this temperature, followed by subsequent cooling, yields a phase distribution dependent on the rate of cooling rather than on previous low-temperature structure.

Table 1. *Structure factors for* α-AgI *at* 150°C

$B=3.5\,\text{Å}^{-2}$

	Hexagonal*		Cubic*		Statistical
hkl	F_o	F_c	F_o	F_c	F_c
111	66·9	64·5	67·1	67·8	67·3
200	119·3	118·1	123·5	123·7	117·9
211	96·0	95·6	97·6	96·7	90·2
220	70·2	70·2	73·9	74·2	79·7
310	57·5	56·9	55·2	55·7	58·2
321	54·8	56·2	64·4	62·5	64·6
400	—		76·2	76·8	77·8

* Designations refer to derivative low-temperature phases.

Radial distribution analysis

The intensity in electron units scattered by a noncrystalline array of atoms at the diffraction angle θ is given by

$$I=\sum_m \sum_n f_m f_n \frac{\sin s r_{mn}}{s r_{mn}} \qquad (1)$$

where $s=4\pi \sin \theta/\lambda$, f_m and f_n are the scattering factors for any two atoms in the structure, and r_{mn} is the interatomic vector. The diffraction pattern from the high-temperature phase of silver iodide, due to the statistical randomization of two silver atoms per unit cell over forty-two available sites, consists of the superposition of the diffraction from a regular array on that from a random structure. The radial distribution function therefore permits the extraction of the information contributed by the random component.

The experimental scattering curves for three different cases, namely those derived from the two low-temperature phases at 150°C after the transition to the stability region of the body-centered cubic phase and a third set derived from data taken at 250°C, were obtained by averaging the data from the applicable runs. The curves obtained with the different X-ray wavelength radiations were adjusted in the overlap region and corrected for polarization and absorption effects. These composite curves were, in turn, fitted to the total independent scattering curve, the sum of the coherent and incoherent scattering curves calculated from the numerical values of the atomic scattering factors, in the high angle region between $s=9$ and $s=11$.

The deviation of the actual electron density $\varrho(r)$ from the mean electron density ϱ_0 for a crystal powder is approximately given by

$$4\pi r^2[\varrho(r)-\varrho_0]=\frac{2r}{\pi}\sum_{s_{\min}}^{s_{\max}} sI(s)\sin rs\Delta s. \qquad (2)$$

The summations were carried out on a high-speed digital computer at intervals of $r=0{\cdot}1$ Å. Computations were carried out both for data including and for data excluding the Bragg peaks, and with varying temperature factors. No significant deviations in results occurred for any of these experimental conditions. A portion of the radial distribution curves over the range of

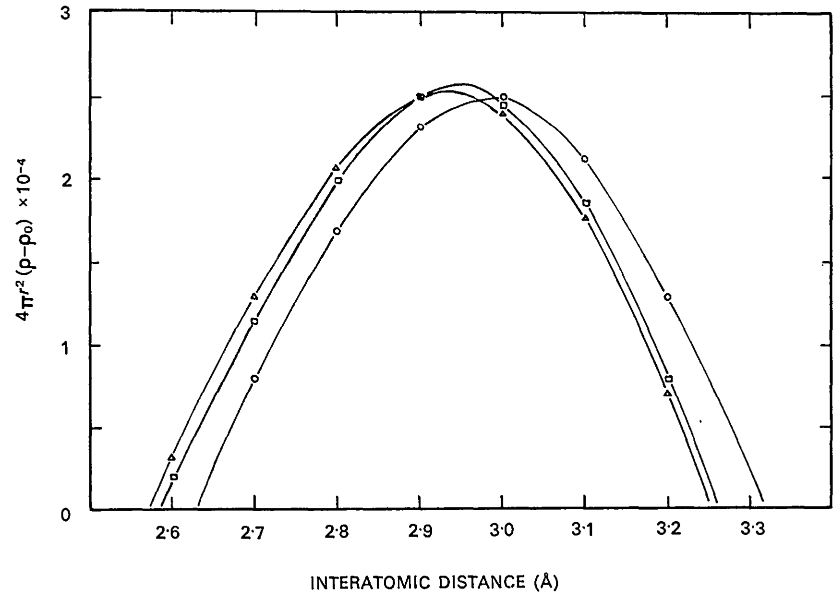

Fig. 1. Radial distribution curves for the high-temperature cubic phase of silver iodide. Triangles and squares represent results for the hexagonal and face-centered cubic derived structures, respectively, heated to 155°C, and circles the results for both at 250°C. (Not corrected for thermal expansion.)

nearest neighbor silver–iodine interatomic distances is shown in Fig. 1.

All curves are broadened by the averaging effect of both nearest neighbor and next nearest neighbor interatomic distances. However, certain features were apparent, and only these will be held to be of any significance. Although reproducible, neither the exact location nor the area under the peaks will be considered, and attention will be focused only on the relative positions of the peaks, defined here as the distances where the numbers of interatomic vectors reach a maximum. These held a constant relation to each other regardless of changes in the experimental parameters previously discussed. For the body-centered cubic phase at 150°C, the average nearest neighbor silver–iodine interatomic distance for those derived from the wurtzite-type hexagonal phase was smaller than that for those derived from the sphalerite-type face-centered cubic phase. When corrected for thermal expansion (Lieser, 1955; Hoshino, 1957) the average nearest neighbor silver–iodine interatomic distance for all structures at 250°C fell midway between the above. Therefore, at temperatures between 147 and 165°C, a negative deviation from the mean interatomic distances exists for those structures derived from the hexagonal low-temperature phase and a positive deviation for those structures derived from the face-centered cubic low-temperature phase. The difference disappears at higher temperatures.

Site occupation analysis

Integrated intensities on a relative scale were obtained from the planimetered areas under all diffraction peaks. Eight independent sets of data were used for each of the averaged values of the intensities from the body-centered cubic phase at 155°C derived from the two low-temperature phases, respectively, and six more for the data at 250°C. All included data points clustered within three per cent of the mean value. The relative intensities were put on an approximately absolute basis by comparison with intensities calculated on the basis of the completely statistical model of Strock (1934, 1936). A Lorentz–polarization correction (*International Tables for X-ray Crystallography*, 1959) and an overall isotropic Debye–Waller temperature factor were applied. The latter was derived graphically from the slope of the curve of the ratio of the observed and calculated intensities against $\sin\theta/\lambda$. Observed structure factor values for the two different experimental conditions are shown in Table 1, and compared with those calculated for the statistical model. Standard deviations for the observed structure factors are estimated at between 0·5 and 0·8% of the given values (Buerger, 1960).

The essential correctness of the model for the structure of the high-temperature phase of silver iodide at 250°C proposed by Strock and more recently confirmed by Hoshino (1957) was assumed in all subsequent calculations. This model places the two iodine atoms in the fixed positions 0,0,0 and $\frac{1}{2},\frac{1}{2},\frac{1}{2}$ of the body-centered cubic unit cell and distributes the two silver atoms statistically over the sixfold sites $0,\frac{1}{2},\frac{1}{2}$ *etc.*, the twelvefold sites $0,\frac{1}{2},\frac{1}{4}$ *etc.*, and the twenty-fourfold sites at $0,x,x$ with $x=\frac{3}{8}$ *etc.* of space group *Im*3*m* (no. 229). The two silver atoms are thus distributed with equal probability over forty-two available lattice sites.

Least-squares calculations were carried out on a high-speed digital computer, holding all atomic positional and temperature parameters constant, to refine on the best values for the silver atom multiplicities on the different equivalent sites. These atom multiplicities are then directly related to the site occupation probabilities. Computations were made both for the case where the multiplicity for atoms in $0,\frac{1}{2},\frac{1}{2}$ was held constant and for the case where the multiplicities for all types of silver atoms was allowed to vary simultaneously, as well as for overall temperature factors $B=2{\cdot}5$ and 3·5 for the data taken at 155°C. The introduction of a third multiplicity variable did not appreciably affect the numerical values for the other two and these results can therefore probably be considered as reliable. In addition to the above, the scale factors were carried as variables throughout. Atomic scattering factors for silver and iodine were interpolated from the tabulated values in *International Tables for X-ray Crystallography* (1962). Results are shown in Table 2, and indicate a preferred occupation probability of silver atoms for sites $0,\frac{1}{2},\frac{1}{4}$ *etc.* for the face-centered cubic derived structure and for sites $0,x,x$ with $x=\frac{3}{8}$ *etc.* for the hexagonal derived structure. Calculated structure factors using these occupancy values are shown in Table 1.

Certain assumptions are implicit in these calculations. These include (1) the maintenance of fixed iodine atom positions, (2) the distribution of silver atoms over the positions of the Strock structure only, (3) the attribution of all observed intensity differences solely to variations in the statistical occupation of entire groups

Table 2. *Least-squares occupation statistics for silver atom sites in the high-temperature* (α) *cubic phase of silver iodide at* 155°C

	Position (Space group *Im*3*m*, no. 229)	Multiplicity	Group occupancy		
			Random (theoretical expectation value)	Hex. derived	f.c.c. derived
Ag(1)	(*b*) $0,\frac{1}{2},\frac{1}{2}$	6	14·4%	2·4%	10·8%
Ag(2)	(*d*) $0,\frac{1}{2},\frac{1}{4}$	12	28·7	26·4	43·2
Ag(3)	(*h*) $0,x,x$ $(x=\frac{3}{8})$	24	57·5	72·0	45·6
				$R=$ 2·5%	1·6%

of equivalent sites and, (4) the use of an overall isotropic temperature factor rather than individual atomic temperature factors.

Discussion

The sum of the silver positions in the structure proposed by Strock (1934, 1936) defines a sphere of exclusion around each iodine atom, and the silver atoms are distributed over the surface of this sphere at roughly equivalent distances from each other. It is obvious that none of the silver sites can be really considered as 'stable' positions, but they nonetheless can be used as volume occupation probability indicators. The Strock model is particularly convenient to use here because it is both easily amenable to treatment by standard crystallographic calculations, and the lack of extensive data precludes the introduction of the many variables required by a more generalized model.

The mechanism for this phase transition can be divided into two aspects, one involving only the iodide ions and the other the more mobile silver ions. A model based primarily on the shift of the iodide ion lattice has been adopted here because both the disparity in ionic sizes (2·16 Å for iodine against 1·26 Å for silver) and the considerably greater mobility of the silver ions suggest that this is the dominant factor. Diagrams indicating the transformation of only the iodine framework, and neglecting the silver atoms, from the face-centered cubic sphalerite-type structure and from the hexagonal wurtzite-type structure are shown in Fig. 2(*a*) and (*b*) respectively. The final iodide ion lattice is identical for both models, and the orientation of the unit cells relative to each other is as follows: f.c.c.[100] = b.c.c.[110] and hex.[110] = b.c.c.[10$\bar{1}$]; hex. [001] = b.c.c.[01$\bar{1}$]. The transition from the face-centered cubic to the body-centered cubic phase probably involves an intermediate tetragonal structure with an axial ratio $c/a=2/\sqrt{2}$, as had been proposed by Strock (1934). A splitting of certain diffraction lines very near the transition temperature was observed in several instances, and appears to confirm this mechanism. The transition from the hexagonal to the body-centered cubic phase, on the other hand, involves both a glide of alternate iodine layers by $\frac{1}{6}$ of the cube face diagonal ([110] hexagonal), or a compensating shift by every layer of half this distance, as well as a small distortion of the iodine framework. However, the total distortion for the hexagonal structure will be less than for the face-centered cubic structure. This, as well as the metastability of the low-temperature face-centered cubic phase, may explain the fact that a certain trend toward conversion to the hexagonal phase on slow cooling through the transition temperature occurs.

The most important crystallographic aspect of this transition, however, involves the silver ions, and a satisfactory explanation for the preceding experimental evidence therefore must be based on a model which differentiates the silver atom site occupation probabilities in the high-temperature phases derived from the two low-temperature phases on the basis of differing preferred configurations. If one considers the distorted low-temperature structures in the framework of the high-temperature body-centered cubic structure the silver atom sites occupied in the low-temperature phases can be shown to lie near permitted sites in the statistical model for the high-temperature phase. Lattice shifts are assumed to be initiated by the iodine atoms, the silver atoms assuming positions of minimum energy in the rearranged unit cell. Essentially, this is equivalent to a lattice distortion of the framework, followed by a relaxation of the interstitials, without breaking any nearest neighbor bonds. Whether the distortion occurs in a single stage or by multiple small successive displacements is not important for this discussion.

In the face-centered cubic structure the silver atoms are located at $\frac{1}{4},\frac{1}{4},\frac{1}{4}$; $\frac{3}{4},\frac{3}{4},\frac{1}{4}$; $\frac{3}{4},\frac{1}{4},\frac{3}{4}$; and $\frac{1}{4},\frac{3}{4},\frac{3}{4}$. Retaining the same origin, in the tetragonal cell these are equivalent to $\frac{1}{2},0,\frac{3}{4}$ and $0,\frac{1}{2},\frac{1}{4}$ and the distortion introduced by the transformation to the body-centered cubic unit cell does not change the relative silver atom positions.

In the hexagonal unit cell the iodine atoms are located at $\frac{1}{3},\frac{2}{3},0$ and $\frac{2}{3},\frac{1}{3},\frac{1}{2}$; the silver atoms at $\frac{1}{3},\frac{2}{3},\frac{5}{8}$ and $\frac{2}{3},\frac{1}{3},\frac{1}{8}$. An opposed shift of $\pm\frac{1}{12}$ (hex. 110) by each of the alternate iodine atom layers, expansion from $c(\text{hex})=4{\cdot}59$ to $c(\text{b.c.c.})=5{\cdot}04$, and a small additional distortion of the iodine framework produces the body-centered cubic structure. If one of the iodine atoms is taken as the new origin the silver atom movement is from initial positions at approximately $\frac{7}{32},\frac{1}{16},\frac{1}{2}$ and $\frac{9}{16},\frac{23}{32},0$ to positions of minimum energy by equalization of bond distances and angles at approximately $\frac{5}{32},\frac{3}{32},\frac{1}{2}$ and $\frac{19}{32},\frac{21}{32},0$. The former are nearest $\frac{1}{4},0,\frac{1}{2}$ and $\frac{1}{2},\frac{3}{4},0$; and the latter nearest $\frac{1}{8},\frac{1}{8},\frac{1}{2}$ and $\frac{5}{8},\frac{5}{8},0$ in the b.c.c. unit cell. The final silver atom positions, in the framework of the structure proposed by Strock, would be equivalent to about a 1:3 ratio of occupation probabilities for the sites at $0,\frac{1}{2},\frac{1}{4}$ *etc.* and at $0,x,x$ with $x=\frac{3}{8}$. The strain relief and consequent shifts of silver atoms may occur in one or more steps. It is important to remember that the experimental data obtained do not give any information on the actual dynamics of the mechanism of the transformation, but only on the

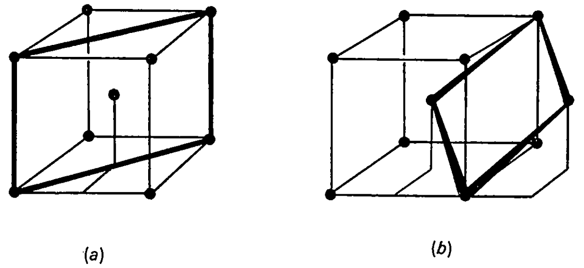
(*a*) (*b*)

Fig. 2. Idealized relationships for the iodine framework in silver iodide. (*a*) The face-centered cubic to body-centered cubic transformation. (*b*) The hexagonal to body-centered cubic transformation.

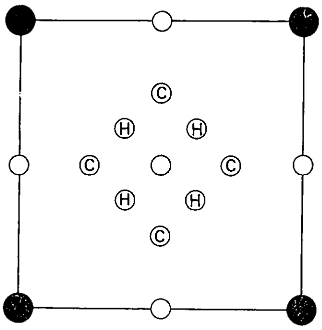

Fig. 3. $z=0$ section of the high-temperature body-centered cubic structure of silver iodide according to Strock (1934, 1936). Open circles represent silver atoms, filled circles iodine atoms. The silver atom sites preferentially occupied in the hexagonal and cubic phase derived structures are indicated.

atomic arrangement in what must be presumed as intermediate states just above the transition temperature at 147°C.

The above would indicate that for the face-centered cubic structure the positions of type $0,\frac{1}{2},\frac{1}{4}$, and for the hexagonal structure the positions $0,x,x$ with $x=\frac{3}{8}$ should be preferentially occupied by virtue of proximity to the final silver sites. As stated earlier, the Strock model merely refers to certain stationary states for highly mobile atoms and deviations from these idealized sites can only be treated as excess thermal motion. The results are not entirely conclusive, moreover, especially for the hexagonal structure because similar experimental results would be obtained if a single actual position is on the average somewhere between $0,\frac{1}{2},\frac{1}{4}$ and $0,\frac{3}{8},\frac{3}{8}$ (but nearer the latter) or if there were a great many positions in that range that were statistically occupied to a higher degree in the hexagonal than in the cubic case. A section of the statistical structure, indicating the preferred sites for the silver atoms in the b.c.c. unit cells derived from the f.c.c. and hexagonal low temperature structures, respectively, is shown in Fig. 3.

On the above basis, if the silver atom distribution is not completely random near the transition temperature but shifted so that sites nearer to the low-temperature analogues are occupied preferentially, then this might account for the tendency to regenerate the respective structures. The memory effect thus is probably due to long-range non-cubic ordering of silver ions, superimposed on considerable short-range disorder. The two different techniques used in this investigation, namely radial distribution and least-squares analysis of site occupation probabilities, appear to confirm this conclusion.

The radial distribution results indicate deviations from the mean interatomic distance of 2·75 Å in the statistical high-temperature b.c.c. structure. For the above described models, the nearest neighbor silver–iodine distances are 2·65 Å for the hexagonal and 2·81 Å for the f.c.c. derived structures, respectively. The observed shift toward a smaller or larger mean interatomic distance is then the result of the preferential weighting of the mean distance of 2·75 Å by the shorter distance due to the hexagonal phase derived structure or to the longer distance due to the f.c.c. derived structure.

The site occupation statistics give a direct indication of the actual weighted silver atom distribution and point to a definite preference for the $0,\frac{1}{2},\frac{1}{4}$ type silver sites for the b.c.c. structure derived from the f.c.c. phase in the temperature region just above the transition point and a somewhat less clearcut preference for the $0,x,x$ with $x=\frac{3}{8}$ type silver sites for the structure derived from the hexagonal phase.

In summary, then, the differentiation of site occupation probabilities based on previous history of the sample appears to be unambiguous, and in accord with the above hypothesis. While certainly not conclusive, the evidence presented here does, however, indicate a trend toward preferential occupation of certain silver atom sites near the transition temperature and this probably accounts for the observed 'memory effect'.

It is a pleasure to thank Mr Dennis Herrin for assistance with the data reduction, Prof. Arthur Bienenstock of Harvard University for valuable discussions concerning the radial distribution method, and Prof. James Stewart of the University of Maryland for assistance on certain phases of the least-squares calculations. These were carried out with the University of Washington–University of Maryland System 63 Program. The author is especially grateful to Dr David P. Shoemaker for many suggestions and comments aimed at clarifying the aims of this paper.

References

Bloch, R. & Moeller, H. (1931). *Z. Phys. Chem.* A. 152, 245.

Burley, G. (1963). *Amer. Min.* **48**, 1266.

Hoshino, S. (1957). *J. Phys. Soc. Japan*, **12**, 315.

International Tables for X-ray Crystallography (1959). Vol. II. p. 270. Birmingham: Kynoch Press.

International Tables for X-ray Crystallography (1962). Vol. III. Birmingham: Kynoch Press.

Lieser, K. H. (1955). *Z. Phys. Chem.* N.F. **5**, 125.

Lieser, K. H. (1956). *Z. Phys. Chem.* N.F. **9**, 302.

Strock, L. W. (1934). *Z. Phys. Chem.* B.**25**, 441.

Strock, L. W. (1936). *Z. Phys. Chem.* B.**31**, 132.

Strock, L. W. (1936). *Z. Kristallogr.* **93**, 285.